2-1-2000

Excitation of Ar 3p^{5}4s-3p^{5}4p Transitions by Electron Impact

Colette M. Maloney

Jerry Peacher
Missouri University of Science and Technology, peacher@mst.edu

Klaus Bartschat

Don H. Madison
Missouri University of Science and Technology, madison@mst.edu

Excitation of Ar $3p^54s$-$3p^54p$ transitions by electron impact

C. M. Maloney,[1] J. L. Peacher,[1] K. Bartschat,[2] and D. H. Madison[1]

[1]*Physics Department, University of Missouri–Rolla, Rolla, Missouri 65409-0640*
[2]*Physics Department, Drake University, Des Moines, Iowa 50311*

Electron-impact excitation of argon from the $3p^54s$ ($J=0,2$) metastable states to the $3p^54p$ ($J=0,1,2,3$) manifold has been investigated in the semirelativistic first-order distorted-wave and plane-wave Born approximations. The results are compared with recent experimental data of Boffard *et al.* [Phys. Rev. A **59**, 2749 (1999)] and *R*-matrix predictions by Bartschat and Zeman [Phys. Rev. A **59**, R2552 (1999)]. In cases for which perturbative approaches are expected to be valid, the plane-wave Born approximation is found to be sufficiently accurate and thus allows for an efficient calculation of results over a wide range of collision energies.

I. INTRODUCTION

Electron scattering from noble gases has been a topic of interest since the very beginning of atomic collision physics. While many features of *e*-He collisions can be described in a nonrelativistic approximation and are now well understood theoretically (see, for example, the recent review by Fursa and Bray [1]), the heavier noble gases (Ne, Ar, Kr, Xe) continue to represent major challenges to both experimentalists and theorists alike. The theoretical problems are mostly due to the relatively difficult description of the excited target spectrum, with a hole in the outermost *p*-shell of the singly excited $np^5n'l$ configurations. As a result, the target states generally have to be treated in a relativistic coupling scheme, and relativistic effects between the projectile electron and the target may be important as well.

In addition to the fundamental challenge posed in the theoretical description of electron collisions with heavy noble gases, the results are also of great importance for many practical applications, particularly in plasma and discharge physics. Due to the difficulties of the measurements, most experimental investigations have concentrated on transitions from the ground state, including elastic scattering, excitation, and ionization processes. (A partial list of references was given, for example, in our earlier work on excitation from the ground state [2].) On the other hand, very few investigations have been devoted to electron collisions with noble gas atoms in excited states, with the notable exception of work on the metastable members of the $(3p^54s)$ manifold in argon. Data for excitation to various levels in the $(3p^54p)$ manifold from the $J=2$ ($1s_5$ in Paschen notation) and $J=0$ ($1s_3$) states were reported by Penkin and co-workers [3,4], and also in recent work by Boffard and co-workers [5–7]. However, major differences in both the energy dependence and the magnitude of the cross sections were reported by the two groups. Note that accurate knowledge of these transitions is again very important for discharge modeling, due to the long lifetimes of the metastable states and the fact that the cross sections for excitation from the metastables can be orders of magnitude larger that those for excitation out of the ground state.

On the theoretical side, results from various semirelativistic Breit-Pauli *R*-matrix (close-coupling) calculations were recently reported by Bartschat and Zeman [8]. For incident electron energies up to approximately 20 eV on the metastable initial states, they obtained reasonable agreement with the data of Boffard *et al.* [7]. On the other hand, some discrepancies remained and the calculations were limited to an energy range near threshold, due to the nature of the *R*-matrix approach used.

The present work is an extension of our earlier study of electron-argon collisions with excitation from the ground state [2]. It was motivated by several goals, namely, (a) to extend the *R*-matrix results to higher energies and thus to provide a comparison with all the experimental data; (b) to study the accuracy of perturbative methods for the description of these collisions, in particular to assess the need for using a distorted-wave model rather than a computationally more efficient plane-wave approach; and (c) to assess the sensitivity of the results on the target description.

II. THEORY

The theoretical approach used here is the semirelativistic first-order distorted-wave approximation of Madison and Shelton [9] and Bartschat and Madison [10], which we will label as SRDW. The details of the theory may be found in the references, so only a brief outline will be presented here. The first-order distorted-wave *T* matrix for atomic excitation is given by

$$T_{fi} = (n+1)\langle \chi_f^-(r_0)\Psi_f(\xi)|V-U_f(r_0)|A\Psi_i(\xi)\chi_i^+(r_0)\rangle. \tag{1}$$

Here *n* is the number of electrons in the atom, r_0 is the coordinate of the incident electron, $\Psi_{i(f)}$ is the initial (final) wave function for the atom with ξ representing the *n* atomic coordinates, *A* is the antisymmetrizing operator for the $(n+1)$ electrons in the problem, U_f is the final-state distorting potential, and *V* is the full interaction between the projectile electron and the atom. The initial-state distorted wave χ_i^+ satisfies an asymptotic outgoing wave boundary condition and the final-state distorted wave χ_f^- satisfies an asymptotic incoming-wave boundary condition. The final-state distorted wave χ_f^- is a solution of Schrödinger's equation

$$(K+U_f-E_f)\chi_f^-=0. \tag{2}$$

Here K is the kinetic-energy operator, E_f the energy of the final-state electron and the distorting potential U_f that contains relativistic effects

$$U_f=\gamma V_f-\tfrac{1}{4}(\alpha V_f)^2-\frac{(j+1)}{r}\frac{\eta'}{\eta}+\frac{3}{4}\left(\frac{\eta'}{\eta}\right)^2-\frac{1}{2}\frac{\eta''}{\eta'}, \tag{3}$$

where

$$\gamma=\sqrt{1+\alpha^2 E_f},$$

$$\eta=1+\gamma-\tfrac{1}{2}\,\alpha^2 V_f. \tag{4}$$

Here V_f is the sum of the spherically symmetric approximation for V and the local approximation of Furness and McCarthy [11] for exchange distortion, α is the fine-structure constant, j takes on the values of either l or $(-l-1)$, where l is the orbital angular momentum of a particular partial wave, and the primes indicate radial derivatives. The initial-state distorted wave χ_i^+ is obtained similarly using the initial-state distorting potential U_i and incident energy E_i. For the present work, we have adopted the practice of using the final-state distorting potential for calculating both the initial-state and final-state distorted waves.

III. RESULTS

We have calculated integral cross sections for electron collisions with an argon atom that has been excited to a metastable state in the $3p^54s$ manifold that corresponds to the $1s$ manifold in the Paschen designation. The two metastable states in this manifold are designated as $1s_5$ ($J=2$) and $1s_3$ ($J=0$), respectively. We have calculated cross sections for exciting seven states with $J=0,1,2,3$ in the $3p^54p$ manifold, which corresponds to the $2p$ manifold in the Paschen designation. In performing these calculations, it has become apparent that a key component for obtaining reliable cross sections is the description of the target. To illustrate this point, we show results obtained from two different sets of atomic wave functions. In our intermediate coupling scheme, a given atomic state is represented as a sum of different electronic configurations; for a given configuration then, a linear combination of all possible contributing LS terms are taken.

The first set of wave functions used corresponds to that applied in the 15-state R-matrix calculation of Bartschat and Zeman [8]. The orbitals and mixing coefficients were generated from the structure code CIV3 of Hibbert [12]. Since mixing effects with the additional target configurations included in the 31-state and 41-state models of Bartschat and Zeman [8] are generally small, and the results of all those models become very similar at higher energies, the simplification of using the 15-state orbitals seemed appropriate for the present work. The 15-state model corresponds to representing the $1s$ manifold by a single configuration ($3p^54s$) and the $2p$ manifold by a single configuration ($3p^54p$). Additional evi-

dence supporting a single configuration representation for these states may be found in our previous distorted-wave calculation for excitation of argon from the ground state [2]. In that work, two configurations ($3p^54p$ and $3p^55p$) were used to represent the $2p$ manifold and it was found that the $5p$ configuration did not affect the cross-section results significantly. In terms of LS states, the nine physical states of interest are expressed in Paschen notation as

$$1s_5=(3p^54s)^3P_2,$$

$$1s_3=(3p^54s)^3P_0,$$

$$2p_9=(3p^54p)^3D_3,$$

$$2p_8=0.827\,687\,1(3p^54p)^3D_2+0.549\,204\,6(3p^54p)^1D_2$$
$$-0.115\,362\,1(3p^54p)^3P_2,$$

$$2p_6=0.374\,685\,1(3p^54p)^3D_2-0.693\,850\,0(3p^54p)^1D_2$$
$$-0.614\,966\,1(3p^54p)^3P_2,$$

$$2p_5=0.976(3p^54p)^3P_0-0.220(3p^54p)^1S_0,$$

$$2p_4=0.514\,325\,4(3p^54p)^3D_1+0.487\,189\,5(3p^54p)^3P_1$$
$$+0.705\,767\,4(3p^54p)^1P_1+0.002\,832\,4(3p^54p)^3S_1,$$

$$2p_3=0.417\,786\,2(3p^54p)^3D_2-0.465\,775\,0(3p^54p)^1D_2$$
$$+0.780\,069\,5(3p^54p)^3P_2,$$

$$2p_2=0.012\,513\,9(3p^54p)^3D_1+0.808\,419\,2(3p^54p)^3P_1$$
$$-0.567\,789\,8(3p^54p)^1P_1+0.154\,649\,8(3p^54p)^3S_1.$$

The second set of wave functions was generated using the SUPERSTRUCTURE (SS) program of Eissner, Jones, and Nussbaumer [13]. The major difference in the SS calculation, as compared to the target description in the CIV3 calculation, lies in the fact that the $3p$ orbital, generated to give the best possible description of the ground state and the $3p^54s$ states, was kept frozen in the optimization of the $4p$ orbital for the members of the $3p^54p$ configuration. In the CIV3 case, on the other hand, several iterations were performed for the $3p$ and $4p$ orbitals to ensure that the $3p$ orbital was also optimized on the $3p^54p$ configuration. The effect of this change will be seen below, but we note already at this point that (a) the present SS description is expected to be inferior to that from CIV3 because of the above change, and (b) if CIV3 and SUPERSTRUCTURE were run with the same optimization criteria, the results would be very similar. In the above SS model, we obtained

$$1s_5=(3p^54s)^3P_2,$$

$$1s_3=(3p^54s)^3P_0,$$

$$2p_9=(3p^54p)^3D_3,$$

TABLE I. Experimental and theoretical oscillator strengths for transitions out of the $1s_5$ and $1s_3$ initial states.

Transition	Wiese et al. [15]	Boffard et al. [7]	CIV3	SS
$1s_5 \rightarrow 2p_9$	0.46 ± 0.04	0.39 ± 0.10	0.46	0.62
$1s_5 \rightarrow 2p_6$	0.214 ± 0.017	0.21 ± 0.05	0.18	0.29
$1s_3 \rightarrow 2p_4$	0.53 ± 0.04	0.38 ± 0.05	0.44	0.73

TABLE II. Experimental and theoretical oscillator strengths for transitions out of the $1s_5$ and $1s_3$ initial states.

Transition	Wiese et al. [15]	CIV3
$1s_5 \rightarrow 2p_8$	0.089 ± 0.007	0.0894
$1s_5 \rightarrow 2p_4$	$0.002\,88 \pm 0.000\,23$	0.0113
$1s_5 \rightarrow 2p_3$	0.0285 ± 0.0023	0.0846
$1s_5 \rightarrow 2p_2$	0.0278 ± 0.0014	0.0378
$1s_3 \rightarrow 2p_2$	0.314 ± 0.016	0.290

$$2p_8 = 0.829\,19(3p^54p)^3D_2 + 0.534\,99(3p^54p)^1D_2$$
$$- 0.161\,97(3p^54p)^3P_2,$$

$$2p_6 = -0.252\,06(3p^54p)^3D_2 + 0.616\,51(3p^54p)^1D_2$$
$$+ 0.745\,91(3p^54p)^3P_2,$$

$$2p_5 = 0.986\,05(3p^54p)^3P_0 + 0.166\,38(3p^54p)^1S_0$$
$$- 0.005\,37(3p^6)^1S_0,$$

$$2p_4 = 0.656\,90(3p^54p)^3D_1 + 0.419\,58(3p^54p)^3P_1$$
$$+ 0.626\,45(3p^54p)^1P_1 + 0.000\,50(3p^54p)^3S_1,$$

$$2p_3 = -0.498\,90(3p^54p)^3D_2 + 0.577\,68(3p^54p)^1D_2$$
$$- 0.646\,05(3p^54p)^3P_2,$$

$$2p_2 = 0.018\,90(3p^54p)^3D_1 + 0.804\,63(3p^54p)^3P_1$$
$$- 0.558\,89(3p^54p)^1P_1 + 0.199\,63(3p^54p)^3S_1.$$

We have included the expressions for $2p_8$ and $2p_2$ for completeness (we performed calculations for all the above states but do not present $2p_8$ and $2p_2$ results in the figures to conserve space). One of the tests for the quality of a wave function is the value it predicts for the optical oscillator strength. One of the experimental methods for obtaining oscillator strengths is to measure cross sections for high enough energy that the Born approximation is valid. In the Born approximation, the high-energy cross sections are proportional to $\ln(E)/E$, where E in the incident energy and the constant of proportionality contains the optical oscillator strength [14]. We have obtained the theoretical oscillator strengths in a similar manner, i.e., we calculated high-energy plane-wave Born (PWBA) results using the wave functions and then found the oscillator strengths from the known high-energy Born behavior. Note that this method neglects the effect of cascading, which, however, is not expected to strongly affect the results of these dominant, optically allowed transitions [7].

In 1989, Wiese et al. [15] critically examined all the oscillator measurements performed for argon and recommended values for many transitions. Table I compares the results of Wiese et al. [15] with our oscillator strengths obtained as described above. Boffard et al. [7] measured cross sections for several transitions from the metastable states in the $1s$ manifold to the $2p$ manifold. Most of these measurements were at low energies where a first-order perturbation model would not be expected to be valid. Three transitions

were investigated for higher energies: $1s_5 \rightarrow 2p_9$ ($J = 2 \rightarrow 3$); $1s_5 \rightarrow 2p_6$ ($J = 2 \rightarrow 2$); and $1s_3 \rightarrow 2p_4$ ($J = 0 \rightarrow 1$). Table I also contains the oscillator strengths of Boffard et al. [7] for these transitions. From the table, it is seen that the CIV3 oscillator strengths are in better agreement with both sets of experiments than the SS predictions. For the $1s_5 \rightarrow 2p_9$ transition, the CIV3 oscillator strength is in excellent agreement with the results of Wiese et al. [15] For the $1s_5 \rightarrow 2p_6$ transition, on the other hand, the two experimental results are in excellent agreement, while the CIV3 results lie within the error bars of the results of Boffard et al. [7] but not the results of Wiese et al. [15]. For the $1s_3 \rightarrow 2p_4$ transition, the CIV3 oscillator strength is between the two experimental values and outside the error bars of both measurements (but closer to that of Boffard et al. [7]). The SS results, on the other hand, do not lie within the error bars for any of the transitions.

Table II compares the CIV3 oscillator strengths with the results of Wiese et al. [15] for the other transitions measured by Boffard et al. [7]. (There are no oscillator strengths listed for Boffard et al. [7] since their measurements for these transitions were for low energy.) It is seen that while the CIV3 results are in reasonable agreement with the experiment for the two stronger transitions ($1s_3 \rightarrow 2p_2$ and $1s_5 \rightarrow 2p_8$), the agreement is much less satisfactory for the weaker transitions.

The present SRDW results for the energy-dependent integrated cross sections for argon are compared with the high-energy measurements of Boffard et al. [7] in Fig. 1. Similar to the comparisons with the optical oscillator strengths, the SRDW results using the CIV3 wave functions are in better agreement with the experiment than results obtained using the SS wave functions. Not surprisingly, the cross-section results mirror those for the optical oscillator strengths if one compares theory with the oscillator strengths of Boffard et al. [7]. For the SS wave functions, the oscillator strengths are larger than the experiment for all three transitions similar to the cross-section results. The CIV3 oscillator strengths, on the other hand, are within the experimental error bars for the $1s_5 \rightarrow 2p_6$ transition and slightly larger than the experiment for the other two transitions—just like the cross-section results. If the oscillator strengths recommended by Wiese et al. [15] are the more accurate, the high-energy experimental cross sections for the $1s_5 \rightarrow 2p_9$ and $1s_3 \rightarrow 2p_4$ are somewhat too small.

In Fig. 2, the SRDW results for the integrated cross sections are compared with nonrelativistic PWBA results. It is seen that the two theories yield essentially the same inte-
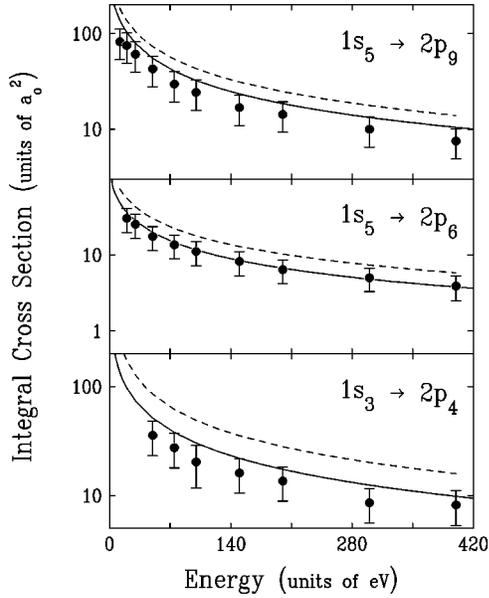
FIG. 1. Integral cross sections for electron-impact excitation of three states in the $2p$ manifold of argon from the metastable states in the $1s$ manifold as a function of incident electron energy. The experimental data are those of Boffard *et al.* [7]. The theoretical SRDW results are SS wave functions (dashed curve) and CIV3 wave functions (solid curve).

grated cross sections above an incident energy of about 20 eV. Since this was not the case for excitations from the ground state [2], effects of distortion, electron exchange, etc., clearly play a less significant role for excitations out of the
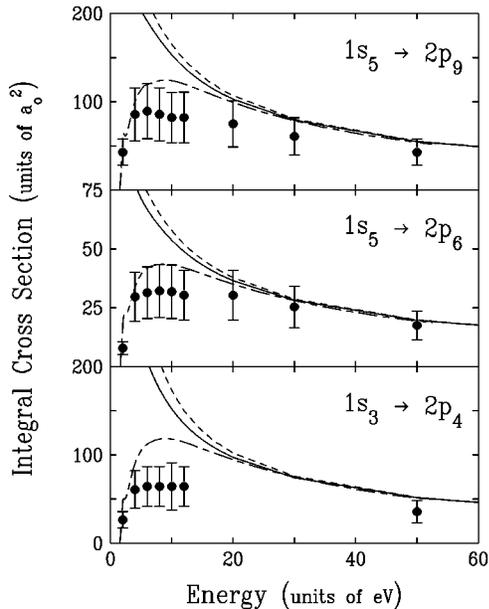

FIG. 2. Integral cross sections for electron-impact excitation of three states in the $2p$ manifold of argon from the metastable states in the $1s$ manifold as a function of incident electron energy. The experimental data are those of Boffard *et al.* [7]. The theoretical results are PWBA (dashed curve); 15-state R-matrix results (long-short dash); and SRDW with CIV3 wave functions (solid curve).

metastable excited states. In fact, it could be argued that there is little reason to perform a more sophisticated first-order calculation than the PWBA since it is known that second- and higher-order terms are important for energies less than about 20–30 eV. As a result, in the energy range where there is a difference between the SRDW and PWBA, the SRDW would most likely be invalid anyhow. As noted above, the Born cross sections are proportional to the optical oscillator strength for high energy. Consequently, in the energy range where the theory is expected to be valid, the quality of the theory depends on the quality of the oscillator strengths, which means the primary theoretical problem reduces to an accurate calculation of the atomic wave functions.

Also shown in Fig. 2 are 15-state R-matrix results. They were obtained by pushing the original calculation of Bartschat and Zeman [8], which uses the same target description as the CIV3 calculation, to higher energies. In order to achieve these results, partial waves up to a total orbital angular momentum $L=30$ were calculated numerically before a geometric series extrapolation was used to estimate the contributions from the higher-L values. We note some differences between the present 15-state results and those published by Bartschat and Zeman [8] due to using a different number of numerical partial waves before extrapolation, and we judge the present results to be more reliable.

As mentioned above, at the higher energies of particular interest for the present work, these 15-state results are very similar to those from the more complex 31-state and 41-state calculations. For higher energies, the R-matrix results must also approach the Born approximation and from the figure it is seen that this occurs at about 30 eV (almost exactly the same energy where the SRDW and PWBA converge). Since the R-matrix calculation contains the strong-coupling effects of all higher terms in a perturbation series calculation (within the target space included in the close-coupling expansion), the difference between the R-matrix and SRDW results indicates the importance of second- and higher-order terms. From Fig. 2, it is seen that higher-order terms are completely unimportant by 30 eV and only significant for energies below 10 eV.

Boffard *et al.* [7] measured six other transitions from the metastable states for incident energies up to 12 eV. Although these energies are clearly too low for a first-order theory to be valid, it is nevertheless interesting to examine these cross sections. In Fig. 3, the R-matrix, PWBA, and SRDW results are compared with the experiment for three of the remaining six transitions. The $1s_5$ level has $J=2$ and the three transitions in the figure correspond to a final state of $J=0$ ($2p_5$), $J=1$ ($2p_4$), and $J=2$ ($2p_3$). The bottom transition ($1s_5 \rightarrow 2p_5$) is optically forbidden and thus there are no PWBA results. Not surprisingly, this cross section is significantly smaller than the optically allowed ones since it results from the exchange amplitude only. Whereas the SRDW is too large in the low-energy region for all the optically allowed transitions, it is too small for the forbidden transition for energies above 5 eV. The R-matrix calculation, on the other hand, is in excellent agreement with the experimental data for the forbidden transition.
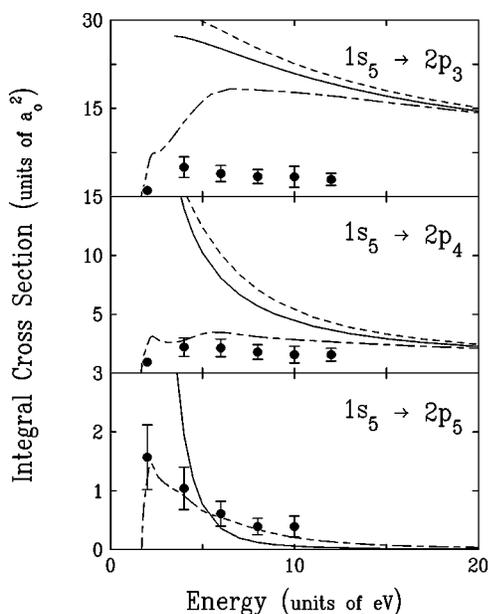
FIG. 3. Same as Fig. 2 except for different atomic states.

From Figs. 2 and 3, it is seen that although the 15-state R-matrix results tend to be in reasonable agreement with the experimental data for the allowed transitions, they are typically a little larger than the data. The notable exceptions are the $1s_5 \rightarrow 2p_3$ and the $1s_5 \rightarrow 2p_2$ (not shown) cases where the discrepancy is much larger. Apparently, channel-coupling effects are relatively more important for these transitions than for others, as can be seen by the significant improvement achieved by the 31-state and 41-state models [8]. For all of the allowed transitions (including the ones not shown), the R-matrix results converge to the SRDW in the 20–30-eV energy range, which indicates convergence to the first term of the perturbation series for these and higher energies.

IV. CONCLUSIONS

We have calculated integrated cross sections for excitation of argon from the two metastable states in the $1s$ manifold to several states in the $2p$ manifold. Boffard *et al.* [7] have measured high-energy cross sections for three optically allowed transitions ($1s_5 \rightarrow 2p_9$, $1s_5 \rightarrow 2p_6$, and $1s_3 \rightarrow 2p_4$), and it was found that first-order perturbation-theory calculations are in good agreement with these data for energies above about 20–30 eV. Further, it was found that the PWBA and SRDW integrated cross-section results were essentially the same for energies above 30 eV, so it is unnecessary to perform a first-order calculation more sophisticated than the plane-wave Born approximation. This observation is in contrast to excitation from the ground state, where distortion effects cannot be ignored in this energy range. Since the Born results depend entirely on the target description, the primary theoretical problem for higher energies reduces to the calculation of the atomic wave functions. We examined two different sets of wave functions and found that the results were very sensitive to the choice. The SS wave functions gave oscillator strengths (and consequently cross sections) that were not in good accord with the experiment, while the CIV3 wave functions, on the other hand, gave oscillator strengths and cross sections in reasonably good agreement with experiment.

Boffard *et al.* [7] also presented several other measurements for energies up to 12 eV, which is too low in energy for a first-order perturbation-theory calculation to be valid. The 15-state R-matrix calculations of Bartschat and Zeman [8] are in reasonable agreement with the low-energy data, and further improvement can be achieved by increasing the number of coupled channels. Comparing the R-matrix and SRDW calculations indicates that higher-order terms in the perturbation series are unimportant for energies greater than 20–30 eV.

[1] D. V. Fursa and I. Bray, J. Phys. B **30**, 757 (1997).

[2] D. H. Madison, C. M. Maloney, and J. B. Wang, J. Phys. B **31**, 873 (1998).

[3] I. Yu. Baranov, N. B. Kolokolov, and N. P. Penkin, Opt. Spektrosk. **58**, 268 (1985) [Opt. Spectrosc. **58**, 160 (1985)].

[4] A. A. Mityureva, N. P. Penkin, and V. V. Smirnov, Opt. Spektrosk. **66**, 790 (1989) [Opt. Spectrosc. **66**, 463 (1989)].

[5] J. B. Boffard, G. A. Piech, M. F. Gehrke, M. E. Lagus, L. W. Anderson, and C. C. Lin, J. Phys. B **29**, L795 (1996).

[6] G. A. Piech, J. B. Boffard, M. F. Gehrke, L. W. Anderson, and C. C. Lin, Phys. Rev. Lett. **81**, 309 (1998).

[7] J. B. Boffard, G. A. Piech, M. F. Gehrke, L. W. Anderson, and C. C. Lin, Phys. Rev. A **59**, 2749 (1999).

[8] K. Bartschat and V. Zeman, Phys. Rev. A **59**, R2552 (1999).

[9] D. H. Madison and W. N. Shelton, Phys. Rev. A **7**, 499 (1973).

[10] K. Bartschat and D. H. Madison, J. Phys. B **20**, 5839 (1987).

[11] J. B. Furness and I. E. McCarthy, J. Phys. B **6**, 2280 (1973).

[12] A. Hibbert, Comput. Phys. Commun. **9**, 141 (1975).

[13] W. Eissner, M. Jones, and H. Nussbaumer, Comput. Phys. Commun. **8**, 270 (1974).

[14] S. Geltman, *Topics in Atomic Collision Theory* (Krieger, Malabar, FL, 1997), p. 112.

[15] W. L. Wiese, J. W. Brault, K. Danzmann, V. Helbig, and M. Kock, Phys. Rev. A **39**, 2461 (1989).